

Open Research Online

The Open University's repository of research publications and other research outputs

Asymptotics of a horizontal liquid bridge

Journal Item

How to cite:

Haynes, M.; O'Brien, S.B.G. and Benilov, E.S. (2016). Asymptotics of a horizontal liquid bridge. *Physics of Fluids*, 28, article no. 042107.

For guidance on citations see [FAQs](#).

© [not recorded]



<https://creativecommons.org/licenses/by-nc-nd/4.0/>

Version: Version of Record

Link(s) to article on publisher's website:
<http://dx.doi.org/doi:10.1063/1.4946001>

Copyright and Moral Rights for the articles on this site are retained by the individual authors and/or other copyright owners. For more information on Open Research Online's data [policy](#) on reuse of materials please consult the policies page.

oro.open.ac.uk

Asymptotics of a horizontal liquid bridge

M. Haynes, S. B. G. O'Brien,^{a)} and E. S. Benilov

*MACSI, Department of Mathematics and Statistics, College of Science and Engineering,
University of Limerick, Limerick, Ireland*

(Received 12 February 2015; accepted 16 March 2016; published online 18 April 2016)

This paper uses asymptotic techniques to find the shape of a two dimensional liquid bridge suspended between two vertical walls. We model the equilibrium bridge shape using the Laplace–Young equation. We use the Bond number as a small parameter to deduce an asymptotic solution which is then compared with numerical solutions. The perturbation approach demonstrates that equilibrium is only possible if the contact angle lies within a hysteresis interval and the analysis relates the width of this interval to the Bond number. This result is verified by comparison with a global force balance. In addition, we examine the quasi-static evolution of such a two dimensional bridge. *Published by AIP Publishing.* [<http://dx.doi.org/10.1063/1.4946001>]

I. INTRODUCTION

The scientific study of liquid surfaces is thought to date from the time of Leonardo da Vinci who experimentally examined the rise of a liquid up a capillarity tube when it is placed in a bath. Later Thomas Young²¹ used the concept of surface tension to explain such capillary rise, also introducing the notion of a contact angle. Some of the original problems which he investigated were solved independently by Laplace and it is for this reason that the capillary equation is often referred to as the Laplace–Young equation. More recently de Gennes, Brochard-Wyart, and Quéré have produced a significant research monograph.⁹

Capillarity forces arise as a result of interfacial forces. If one considers a free surface between air and water, the water molecules in the fluid bulk are surrounded by attractive neighbours, while molecules in the surface are attracted by a reduced number of neighbours and are thus in an energetically unfavourable state. The creation of new surface is energetically costly, and a fluid system will act to minimize surface areas. Interfacial or surface tension is thus a material property of a free surface resulting from the different attractive intermolecular forces that act in the two phases. The result is an interfacial energy per unit area which acts to resist the creation of new interface: in a continuum sense this is equivalent to a tension acting in all directions parallel to the interface.

The Laplace–Young equation can be derived via energy minimisation or via an interfacial force balance. The terms in the Laplace–Young capillary equation can thus be interpreted as representing pressure, gravity, and surface tension effects. Due to the general intractability of the non-linear equation, the usual approach to such problems has been either numerical or asymptotic.^{1,5,6,20} There is a considerable literature on liquid drops and bridges,⁴ and, in the absence of exact solutions, particular attention has been paid to asymptotic solutions and the analysis of steady states and stability and the smaller literature on non-axisymmetric problems.^{10,19} The asymptotic approach has the obvious advantage of allowing one to probe the structure of the solutions,^{12,14} especially, as in the present paper, when multiple solutions are available if the drop or bridge is parameterised by its volume. However, in order to do this, it is necessary to obtain formal perturbation solutions to at least the first order in the small parameter. A leading order analysis as suggested by many authors (based on small Bond number) is insufficient.

In the present paper, we construct an asymptotic solution for the shape of a static liquid bridge, hanging horizontally, supported by two vertical walls. We first demonstrate that a straightforward

^{a)} Author to whom correspondence should be addressed. Electronic mail: stephen.obrien@ul.ie

approach to obtaining asymptotic solutions to first order fails due to the complicated nature of the leading order solutions. It is for this reason, apparently, that though many authors make reference to leading order, constant curvature, approximations,⁴ a first order approximation has not yet been recorded. A leading order analysis allows equilibrium configurations in the case of the contact angle being constant. But it is by proceeding to first order that it becomes clear that equilibrium only occurs if contact angle hysteresis is permitted, and the width of the hysteresis interval is found to be of the same order of magnitude as the Bond number in the asymptotic theory. This motivates us, in Section II, to reformulate the problem using a parametrization, first suggested by Thomas Young in 1805,²¹ and similar to that used by Finn⁶ and O'Brien.^{13,15,16} This has the advantage that the leading order solutions have a sufficiently simple form that extension to higher order is feasible. More recently, Finn *et al.*^{7,8,3} have used this formulation to form a complete integral to explicitly represent solutions in a uniform gravity field.

In Section II we formulate and scale the problem using the Laplace–Young equation. In Section IV we find approximate solutions based upon small Bond number. In Section V we compare the results of asymptotic series with a numerical solution of the equations. In Section VI we provide a description of the quasi-static evolution of the fluid bridge as the volume of liquid decreases due to evaporation. Finally, in Section VII, we discuss the liquid bridges which arise during the manufacture of stents, and how the present work might be extended to physically more interesting configurations.

II. FORMULATION

We consider a liquid bridge such as in Figure 1. The common form of the Laplace–Young equation is²

$$\Delta p = -\sigma \mathcal{K}, \quad (2.1)$$

where \mathcal{K} is the curvature of the fluid surface, and Δp is the pressure difference across the interface. Referring to Figure 1, we note that the pressure at the surfaces at $z = h_{\pm}(x)$ is given by

$$p = \mp \sigma \frac{\frac{d^2 h_{\pm}}{dx^2}}{\left[1 + \left(\frac{dh_{\pm}}{dx}\right)^2\right]^{\frac{3}{2}}}, \quad (2.2)$$

where σ is the surface tension. In the static case, the Navier-Stokes equations give us

$$\frac{dp}{dz} = -\rho g, \quad (2.3)$$

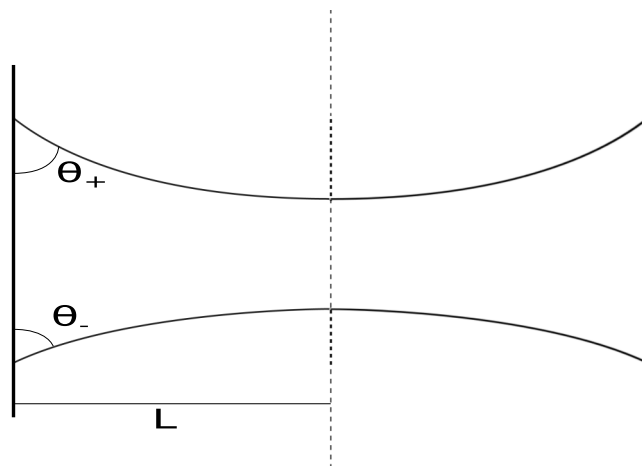


FIG. 1. A sketch of the model geometry, with gravity vertically acting downwards.

and so, the pressure is hydrostatic and is given by

$$p = -\rho g z + P, \quad (2.4)$$

where P is a constant to be determined. Thus combining these two equations we find that

$$-\rho g h_{\pm} + P = \mp \sigma \frac{\frac{d^2 h_{\pm}}{dx^2}}{\left[1 + \left(\frac{dh_{\pm}}{dx}\right)^2\right]^{\frac{3}{2}}}. \quad (2.5)$$

A. Boundary conditions

We refer to Figure 1. Examination of Equation (2.5) suggests that we require a total of five boundary conditions: two for h_+ , two for h_- and one to fix the constant P . We use the boundary conditions that the interfaces meet the wall at a known contact angle and a symmetry condition (the profile is always flat in the centre between the two walls). Hence we obtain the four boundary conditions

$$\left. \frac{dh_{\pm}}{dx} \right|_{x=0} = \mp \cot \theta_{\pm}, \quad (2.6)$$

$$\left. \frac{dh_{\pm}}{dx} \right|_{x=L} = 0, \quad (2.7)$$

where L is the half-width (see Figure 1) and θ_{\pm} is the contact angle between the interface h_{\pm} and the wall at $x = 0$. The final boundary condition is chosen to fix our axes. We set that $h_+(L) = 0$ to make the algebra of the problem easier, without loss of generality.

B. Scaling

As we described earlier, we wish to use asymptotic techniques to obtain a series solution. We introduce the nondimensional variables \tilde{x} and \tilde{z} such that

$$x = L\tilde{x}, \quad h_{\pm} = L\tilde{h}_{\pm}. \quad (2.8)$$

Applying this to (2.5) we find (after dropping the tildes)

$$-Bh_{\pm} + P = \mp \frac{\frac{d^2 h_{\pm}}{dx^2}}{\left[1 + \left(\frac{dh_{\pm}}{dx}\right)^2\right]^{\frac{3}{2}}}, \quad (2.9)$$

where $B \equiv \rho g L^2 / \sigma$ is the Bond number, ρ, g, L, σ being, respectively, the liquid density, gravitational acceleration, characteristic length scale and surface tension. Applying this scaling to the boundary conditions they become

$$\left. \frac{dh_{\pm}}{dx} \right|_{x=0} = \mp \cot \theta_{\pm}, \quad \left. \frac{dh_{\pm}}{dx} \right|_{x=1} = 0, \quad h_+(1) = 0. \quad (2.10)$$

For the stents in question the typical length scale is small (~ 1 mm), so we assume here that the Bond number is small. For example, if the fluid is water at 20°C the Bond number would be approximately 0.25. As such we use it as the small parameter in our asymptotic series. In Appendix A we see asymptotic solutions of this form are very difficult, if not impossible, to find. Hence, following a similar method to that used by O'Brien,¹⁷ we look for an alternative mathematical formulation of the problem.

III. A PARAMETRIC FORMULATION

An alternative formulation of the problem uses the inclination, ϕ, x, h_{\pm} , as dependent variables, depending on the arclength measured from $x = 0$, s . In this formulation (2.5), the Laplace–Young

equation is

$$\frac{d\phi}{ds} - Bh = P, \quad (3.1)$$

$$\frac{dx}{ds} = \cos \phi, \quad (3.2)$$

$$\frac{dh}{ds} = \sin \phi. \quad (3.3)$$

We can eliminate the arclength from this system and obtain

$$\frac{dx_{\pm}}{d\phi} = \frac{\cos \phi}{Bh + P}, \quad (3.4)$$

$$\frac{dh_{\pm}}{d\phi} = \pm \frac{\sin \phi}{Bh + P}. \quad (3.5)$$

Here we consider x_{\pm} and h_{\pm} to be dependent variables, with the inclination, ϕ as the independent variable.

A. Parametric boundary conditions

In this formulation, boundary conditions (2.6) become

$$x_+(0) = 1, \quad x_+(\alpha_+) = 0, \quad h_+(0) = 0, \quad (3.6)$$

on the upper interface and

$$x_-(0) = 1, \quad x_-(\alpha_-) = 0, \quad (3.7)$$

on the lower interface, where α_{\pm} is the surface inclination at the wall, which we can relate to the contact angle θ_{\pm} by $\alpha_{\pm} = \theta_{\pm} - \pi/2$. Thus we have four boundary conditions for each of the four equations corresponding to (3.4) and (3.5) and one extra condition to fix the unknown pressure P .

IV. ASYMPTOTIC SERIES SOLUTIONS OF THE PARAMETRIC EQUATIONS

As asymptotic series solutions in Appendix A we take the Bond number to be the small parameter. Again, we assume solutions of the form:

$$x_{\pm} = x_{\pm}^{(0)} + Bx_{\pm}^{(1)} + B^2x_{\pm}^{(2)} + O(B^3), \quad (4.1)$$

$$h_{\pm} = h_{\pm}^{(0)} + Bh_{\pm}^{(1)} + B^2h_{\pm}^{(2)} + O(B^3). \quad (4.2)$$

Recall that x_{\pm} and h_{\pm} are now functions of ϕ . With some foresight we assume the lower contact angle is only slightly different from the upper contact angle, i.e., $\alpha_- = \alpha_+ + Bc$ where c is a constant to be determined with $c = c^{(0)} + Bc^{(1)} + O(B^2)$. This could be inferred from (4.43) in the case when $B \ll 1$. With this we obtain the boundary condition

$$x_-(\alpha_+ + Bc) = 0. \quad (4.3)$$

We expand this boundary condition in a Taylor series about $\phi = \alpha_+$ to obtain

$$x_-(\alpha_+) + Bc \left. \frac{dx_-}{d\phi} \right|_{x=\alpha_+} + \frac{B^2c^2}{2} \left. \frac{d^2x_-}{d\phi^2} \right|_{x=\alpha_+} + O(B^3) = 0. \quad (4.4)$$

Therefore

$$x_-(\alpha_+) \sim -Bc \left. \frac{dx_-}{d\phi} \right|_{x=\alpha_+} - \frac{B^2c^2}{2} \left. \frac{d^2x_-}{d\phi^2} \right|_{x=\alpha_+}. \quad (4.5)$$

To solve for c we require a further condition. Here we use the condition that the dimensionless height of the bridge at the centre is known (i.e., the minimum dimensionless height of the bridge), and we label this distance b . Thus we have the condition $h_-(\phi = 0) = -b$. An alternative approach would have been to assume that the volume is known and then to calculate c using (4.43).

A. Leading order

When we consider $O(1)$ terms, (3.4) and (3.5) yield

$$\frac{dh_+^{(0)}}{d\phi} P^{(0)} - \sin \phi = 0, \quad (4.6)$$

$$\frac{dx_+^{(0)}}{d\phi} P^{(0)} - \cos \phi = 0, \quad (4.7)$$

$$h_+^{(0)} = 0, \text{ for } \phi = 0, \quad (4.8)$$

$$x_+^{(0)} = 1, \text{ for } \phi = 0, \quad (4.9)$$

$$x_+^{(0)} = 0, \text{ for } \phi = \alpha_+. \quad (4.10)$$

Solving this system we find that

$$h_+^{(0)} = \frac{\cos \phi - 1}{\sin \alpha_+}, \quad (4.11)$$

$$x_+^{(0)} = \frac{\sin \alpha_+ - \sin \phi}{\sin \alpha_+}, \quad (4.12)$$

$$P^{(0)} = -\sin \alpha_+, \quad (4.13)$$

which gives the leading order behaviour for the upper surface. Then using the obtained value for $P^{(0)}$ the lower surface system becomes

$$\frac{dh_-^{(0)}}{d\phi} \sin \alpha_+ = \sin \phi, \quad (4.14)$$

$$\frac{dx_-^{(0)}}{d\phi} \sin \alpha_+ + \cos \phi = 0, \quad (4.15)$$

$$h_-^{(0)} = -b, \text{ for } \phi = 0, \quad (4.16)$$

$$x_-^{(0)} = 1, \text{ for } \phi = 0. \quad (4.17)$$

This yields the leading order solution

$$h_-^{(0)} = \frac{1 - \cos \phi}{\sin \alpha_+} - b, \quad (4.18)$$

$$x_-^{(0)} = \frac{\sin \alpha_+ - \sin \phi}{\sin \alpha_+}. \quad (4.19)$$

B. 1st order

If we now consider terms of $O(B)$, (3.4) and (3.5) then leave

$$\frac{dh_{\pm}^{(0)}}{d\phi} (h_{\pm}^{(0)} + P^{(1)}) + \frac{dh_{\pm}^{(1)}}{d\phi} P^{(0)} = 0, \quad (4.20)$$

$$\frac{dx_{\pm}^{(0)}}{d\phi} (h_{\pm}^{(0)} + P^{(1)}) + \frac{dx_{\pm}^{(1)}}{d\phi} P^{(0)} = 0, \quad (4.21)$$

with the boundary conditions,

$$h_{\pm}^{(1)}(0) = 0, \quad x_+^{(1)}(0) = 0, \quad (4.22)$$

$$x_+^{(1)}(\alpha_+) = 0, \quad x_-^{(1)}(\alpha_+) = -c^{(0)} \frac{dx_-^{(0)}}{d\phi} \Big|_{\phi=\alpha_+}. \quad (4.23)$$

To fix $c^{(0)}$ we use the condition $x_-^{(1)}(0) = 0$. We can solve this system to obtain the solutions

$$h_+^{(1)} = \frac{1}{2 \sin^3 \alpha_+} (\cos^2 \phi - \cos \phi \cos \alpha_+) \quad (4.24)$$

$$+ \frac{1}{2 \sin^4 \alpha_+} (\alpha_+ (1 - \cos \phi)) + \frac{\cos \alpha_+ - 1}{2 \sin^3 \alpha_+},$$

$$x_+^{(1)} = -\frac{1}{2 \sin^3 \alpha_+} (\sin \phi (\cos \phi - \cos \alpha_+)) \quad (4.25)$$

$$+ \frac{\alpha_+ \sin \phi}{\sin^4 \alpha_+} - \frac{\phi}{2 \sin^3 \alpha_+},$$

$$h_-^{(1)} = \frac{1}{\sin^2 \alpha_+} (b(\cos \phi - 1)) \quad (4.26)$$

$$+ \frac{1}{2 \sin^3 \alpha_+} ((\cos \alpha_+ - 4) \cos \phi + \cos^2 \phi)$$

$$+ \frac{1}{2 \sin^4 \alpha_+} (\alpha_+ \cos \phi - \alpha_+) + \frac{3 - \cos \alpha_+}{2 \sin^3 \alpha_+},$$

$$x_-^{(1)} = \frac{1}{2 \sin^4 \alpha_+} ((2b \sin^2 \alpha_+ + \alpha_+) \sin \phi) \quad (4.27)$$

$$+ \frac{1}{2 \sin^3 \alpha_+} ((\cos \alpha_+ + \cos \phi - 4) \sin \phi + \phi),$$

$$P^{(1)} = -\frac{\sin \alpha_+ \cos \alpha_+ + \alpha_+ - 2 \sin \alpha_+}{2 \sin^2 \alpha_+}, \quad (4.28)$$

$$c^{(0)} = \frac{\alpha_+ \sin \alpha_+ (\cos \alpha_+ - 2) + b \sin^2 \alpha_+}{\sin^2 \alpha_+ \cos \alpha_+}. \quad (4.29)$$

For the configuration of the bridge to be in its limiting state (when the upper and lower interfaces just meet at the centre) we set $b = 0$ in Equations (4.24)-(4.29). For the upper surface, in Figure 2 we can compare the two asymptotic series solutions up to first order.

C. 2nd order

The system at 2nd order, $O(B^2)$, is

$$\frac{dh_{\pm}^{(0)}}{d\phi} (h_{\pm}^{(1)} + P^{(2)})$$

$$+ \frac{dh_{\pm}^{(1)}}{d\phi} (h_{\pm}^{(0)} + P^{(1)}) = -\frac{dh_{\pm}^{(2)}}{d\phi} P^{(0)}, \quad (4.30)$$

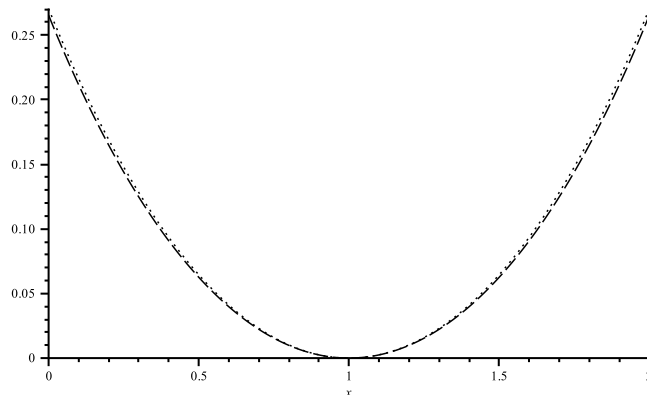


FIG. 2. Comparison of the series solutions given in Appendix A (dot) and Sec. IV (dash) series solutions to first order.

and on the lower surface

$$\begin{aligned} & \frac{dx_{\pm}^{(0)}}{d\phi}(h_{\pm}^{(1)} + P^{(2)}) \\ & + \frac{dx_{\pm}^{(1)}}{d\phi}(h_{\pm}^{(0)} + P^{(1)}) = -\frac{dx_{\pm}^{(2)}}{d\phi}P^{(0)}, \end{aligned} \quad (4.31)$$

with boundary conditions

$$h_{\pm}^{(2)}(0) = 0, \quad (4.32)$$

$$x_{+}^{(2)}(0) = 0, \quad (4.33)$$

$$x_{+}^{(2)}(\alpha_{+}) = 0, \quad (4.34)$$

$$\begin{aligned} x_{-}^{(2)}(\alpha_{+}) = & -c^{(0)} \left. \frac{dh_{-}^{(1)}}{d\phi} \right|_{\phi=\alpha_{+}} + c^{(1)} \left. \frac{dh_{-}^{(0)}}{d\phi} \right|_{\phi=\alpha_{+}} \\ & - \frac{1}{2} \left(c^{(0)} \right)^2 \left. \frac{d^2 h_{-}^{(0)}}{d\phi^2} \right|_{\phi=\alpha_{+}}. \end{aligned} \quad (4.35)$$

We then fix $c^{(1)}$ using $x_{-}^{(2)}(0) = 0$. Using our results from the previous sections, we obtain

$$\begin{aligned} 4 \sin^{11} \alpha_{+} h_{+}^{(2)} = & -H_{21}^{+} - H_{22}^{+} \cos \phi \\ & - H_{23}^{+} \cos^2 \phi \\ & - H_{24}^{+} \cos^3 \phi, \end{aligned} \quad (4.36)$$

$$\begin{aligned} x_{+}^{(2)} = & X_{21}^{+} \phi + X_{22}^{+} \sin \phi + X_{21}^{+} \sin \phi \cos \phi \\ & + X_{23}^{+} \sin \phi \cos^2 \phi, \end{aligned} \quad (4.37)$$

$$\begin{aligned} 4 \sin^7 \alpha_{+} h_{-}^{(2)} = & H_{21}^{-} (1 - \cos \phi) \\ & + \frac{H_{22}^{-}}{2} \sin^2 \phi \\ & + \frac{H_{23}^{-}}{3} (1 - \cos^3 \phi), \end{aligned} \quad (4.38)$$

$$\begin{aligned} 4 \sin^7 \alpha_{+} x_{-}^{(2)} = & \left(X_{21}^{-} + \frac{3X_{23}^{-}}{4} \right) \sin \phi \\ & + X_{22}^{-} (\phi + \sin \phi \cos \phi) \\ & + \frac{X_{23}^{-}}{3} \sin \phi \cos^2 \phi, \end{aligned} \quad (4.39)$$

$$\begin{aligned} 2 \sin^5 \alpha_{+} P^{(2)} = & \alpha_{+}^2 - \sin^2 \alpha_{+} + \cos \alpha_{+} \sin^2 \alpha_{+} \\ & + 2 \alpha_{+} \sin \alpha_{+} \cos \alpha_{+} \\ & - \alpha_{+} \sin \alpha_{+}. \end{aligned} \quad (4.40)$$

Here the X_{2i}^{\pm} and H_{2j}^{\pm} are constants (with a dependence on the upper contact angle θ_{+} only), given in [Appendix B](#). Again, if we want to obtain the configuration of the bridge in its limiting state we must set $b = 0$ in Equations (4.36)-(4.40). In addition, the details of $c^{(1)}$ can be found in [Appendix B](#).

D. Contact angle hysteresis

We note that the asymptotic solutions indicate that, at leading order, the upper and lower angles θ_{+} , θ_{-} must be equal or no solution is possible. This is reasonable because at leading order (i.e., for $B = 0$), gravity plays no role, the liquid bridge is perfectly symmetrical and the upper and lower curves are both circular arcs. Proceeding to the next order, we note that equilibrium now requires that $\theta_{+} < \theta_{-}$, and this corroborates the ansatz in (4.3).

We can verify these results by considering an exact force balance on the liquid bridge in Figure 1. The liquid half-volume can be found by integrating over the half-bridge whence we obtain

$$V = \int_0^1 \int_{h_-}^{h_+} dz dx = \int_0^1 \{h_+ - h_-\} dx. \quad (4.41)$$

However using Equation (2.9) this yields

$$\begin{aligned} BV &= \int_0^1 \left\{ \frac{\frac{d^2 h_+}{dx^2}}{\left[1 + \left(\frac{dh_+}{dx}\right)^2\right]^{\frac{3}{2}}} \right\} dx \\ &\quad + \int_0^1 \left\{ \frac{\frac{d^2 h_-}{dx^2}}{\left[1 + \left(\frac{dh_-}{dx}\right)^2\right]^{\frac{3}{2}}} \right\} dx, \\ &= \left[\frac{\frac{dh_+}{dx}}{\left[1 + \left(\frac{dh_+}{dx}\right)^2\right]^{\frac{1}{2}}} + \frac{\frac{dh_-}{dx}}{\left[1 + \left(\frac{dh_-}{dx}\right)^2\right]^{\frac{1}{2}}} \right]_0^1 \\ &= (\cos \theta_+ - \cos \theta_-). \end{aligned} \quad (4.42)$$

$$= (\cos \theta_+ - \cos \theta_-). \quad (4.43)$$

Here we have exploited the symmetry about $x = 1$ so that V is the half-volume of the bridge. This imposes an equilibrium relation between the upper and lower contact angles. This can also be interpreted as a statement that the weight of the bridge is supported by the upward component of the surface tension at the edges. The vertical walls exert a reaction force equal to the tangential component of the surface tension force at the points (lines) of contact. Specifically, the half-weight of the liquid is $\rho g V$ per unit length in the in-plane direction, while the net surface tension force in the vertical direction per unit length is $\sigma(\cos \theta_+ - \cos \theta_-)$. Hence, in order to get a net upward force, the upper and lower angles must be unequal (in the case of equilibrium), with $\theta_+ < \theta_-$, this difference being accounted for by the occurrence of contact angle hysteresis.

For a perfectly flat clean surface it is generally suggested that there is precisely one equilibrium contact angle. But real surfaces tend to be non-flat and chemically impure and this gives rise to a range of possible contact angles values. Referring to Figure 3, the most up-to-date theory (see also, Refs. 9 and 11) is that when a contact line is moving with speed U_{sl} , the contact angle assumes at the least its maximal (advancing) value $\theta = \theta_a$ for $U_{sl} > 0$ and at the most its minimal (receding) value $\theta = \theta_r$ for $U_{sl} < 0$. When $U_{sl} = 0$, the contact angle can take a range of values with $\theta \in (\theta_r, \theta_a)$ and it is this hysteretic range which allows equilibrium solutions in the present problem. For example, let us consider a small spherical droplet resting on a horizontal surface. If

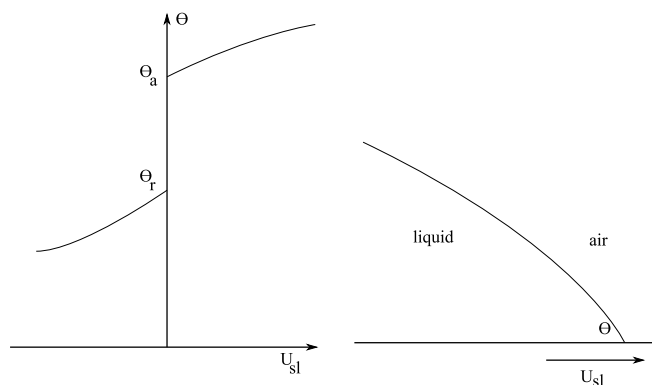


FIG. 3. Contact angle hysteresis as the contact line velocity varies.

liquid evaporates from the droplet, it decreases in volume and contact angle, maintaining the same contact area with the underlying surface until it begins to recede. The contact line then recedes with a constant contact angle, θ_r , characteristic of the surface chemistry and topography. If liquid is added to the drop, it “advances” with contact angle θ_a .

We now verify the solutions given earlier by finding $c^{(0)}$ and $c^{(1)}$ by using the exact result (4.43). Thus we substitute

$$\theta_- = \theta_+ + c^{(0)}B + c^{(1)}B^2 + O(B^3) \quad (4.44)$$

into (4.43) to obtain

$$\begin{aligned} c^{(0)} &= \frac{V^{(0)}}{\sin \theta_+} = \frac{V^{(0)}}{\cos \alpha_+}, \\ c^{(1)} &= \frac{V^{(1)}}{\sin \theta_+} - \frac{V^{(0)2} \cos \theta_+}{2 \sin^3 \theta_+} \\ &= \frac{V^{(1)}}{\cos \alpha_+} + \frac{V^{(0)2} \sin \alpha_+}{2 \cos^3 \alpha_+}. \end{aligned} \quad (4.45)$$

Now we return to (4.41) which we rewrite as

$$V = \int_{\alpha_+}^0 h_+ \frac{dx_+}{d\phi} d\phi - \int_{\alpha_-}^0 h_- \frac{dx_-}{d\phi} d\phi. \quad (4.46)$$

We expand this in an asymptotic series to obtain

$$V^{(0)} = \int_{\alpha_+}^0 \left(h_+^{(0)} \frac{dx_+^{(0)}}{d\phi} - h_-^{(0)} \frac{dx_-^{(0)}}{d\phi} \right) d\phi, \quad (4.47)$$

$$\begin{aligned} V^{(1)} &= \int_{\alpha_+}^0 \left(h_+^{(0)} \frac{dx_+^{(1)}}{d\phi} + h_+^{(1)} \frac{dx_+^{(0)}}{d\phi} \right) d\phi \\ &\quad + \int_{\alpha_+}^0 \left(-h_-^{(0)} \frac{dx_-^{(1)}}{d\phi} - h_-^{(1)} \frac{dx_-^{(0)}}{d\phi} \right) d\phi + c^{(0)} \left(h_-^{(0)} \frac{dx_-^{(0)}}{d\phi} \right) \Big|_{\phi=\alpha_+}. \end{aligned} \quad (4.48)$$

Applying the leading order results and (4.24)–(4.29) we find

$$\sin^2 \alpha_+ V^{(0)} = b \sin^2 \alpha_+ + \cos \alpha_+ \sin \alpha_+ - 2 \sin \alpha_+ + \alpha_+, \quad (4.49)$$

and $V^{(1)}$ can be found in Appendix B. When we substitute these values into (4.45) we obtain the same values for $c^{(0)}$ and $c^{(1)}$ as given in (4.29) and (B1).

E. Limiting volume

Using Equations (4.49) and (B2) we can construct a first order asymptotic series approximation for the limiting volume of the fluid bridge (i.e., the smallest possible bridge as determined by the Laplace–Young equation which occurs when the upper and lower surfaces just touch in the centre), namely,

$$V_{\text{crit}} = V^{(0)} \Big|_{b=0} + B V^{(1)} \Big|_{b=0}, \quad (4.50)$$

which we can then compare with the value given by numerical computation, see Table I. We see that this first order series yields a good approximation to the limiting volume.

V. COMPARING NUMERICAL AND ASYMPTOTIC RESULTS

To verify the asymptotic solutions, we can use the formulation (2.9) or (3.4) and (3.5). Using the former we note that we can obtain numerical solutions if we know the upper contact angle and one of the following three; lower contact angle, volume, distance between the two interfaces half-way between the walls.

TABLE I. Table comparing the asymptotic and numerical limiting volumes of the fluid bridge for $\theta_+ = \pi/3$ for Bond numbers up to 1.

B	Volume given by (4.50)	Numerical volume
0.1	0.1703	0.1703
0.5	0.1572	0.1584
1	0.1408	0.1454

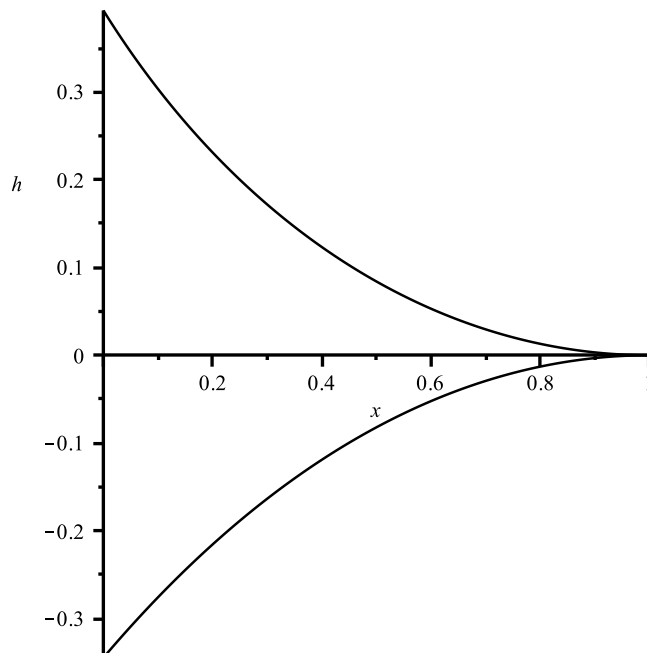
If we know the lower contact angle then we can solve the system numerically with no analytic work required, since here we have two second order ordinary differential equations and one arbitrary constant P with five boundary conditions (2.10). If we know the volume of the bridge (here we really mean half-volume, as in Section IV D) then we can find the lower contact angle from Equation (4.43) and proceed in the same way. If instead, we know the distance between the two interfaces at $x = 1$, then we can use this as a sixth boundary condition and set volume as a second free constant which will fix the lower contact angle. In practice it may be experimentally easiest to measure the centre distance between the two interfaces so we consider this case for the remainder of this work.

We now solve this system numerically over the half-length of the bridge: this requires solution of a boundary value problem. Figure 4 shows the numerical solution for $\theta_+ = \pi/4$, $B = 0.5$ and $b = 0$. Of course the numerical solution holds for all values of the Bond number.

Using these numerical solutions we can now examine the validity of the asymptotic series results. Figure 5 shows the asymptotic series solution plotted with the numerical solution for $\theta_+ = \pi/4$ and $B = 0.5$ in the limiting case when $b = 0$. We see that the asymptotic series solution is in very good agreement with the numerical solution.

VI. QUASI-STATIC EVOLUTION OF THE BRIDGE

Here we briefly sketch (starting in Figure 6) an example of the evolution of a bridge as liquid is removed, for example, by evaporation. In particular, we assume that the time scale for the evaporation is much slower than that for the free surface equilibration so that a quasi-static approximation is

FIG. 4. Numerical solution for the limiting bridge with $\theta_+ = \pi/4$ and $B = 0.5$.

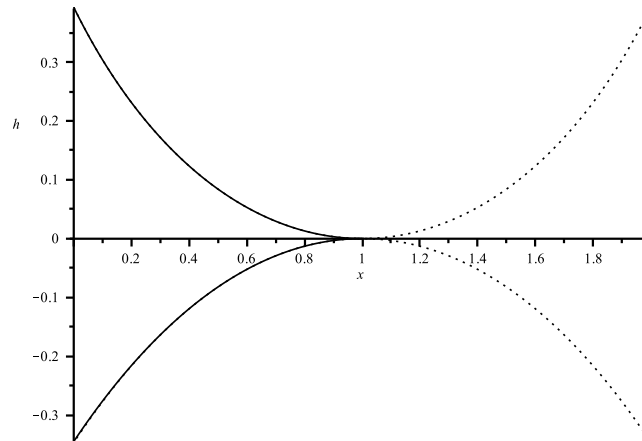


FIG. 5. Numerical solution (full line) and second order asymptotic solution (dotted line) for $\theta_+ = \pi/4$, $B = 0.5$, and $b = 0$.

appropriate. Consider a liquid bridge held between two identical substrates with hysteresis interval $(\theta_r, \theta_a) = (\pi/4, \pi/2)$ as in Figure 7. While this is a large hysteresis interval, it is not unreasonable for a rough surface to have an interval this large. We take the liquid bridge to have lower contact angle close to $\theta_a = \pi/2$. Both contact angles must be inside the hysteresis interval and satisfying (4.43). Therefore the triple points are “pinned.” When the volume is reduced we find both contact angles decrease (see Figure 6), while still satisfying (4.43). As we continue to remove liquid both contact angles will continue to decrease until $\theta_+ = \theta_r$ (Fig. 8). At this point if the volume continues to be reduced the upper triple point becomes “unpinned” and the configuration is no longer static. The upper triple point will travel down the substrate until either the volume stops decreasing or the limiting bridge is reached. If liquid is removed from the limiting bridge, the bridge (as predicted by the Laplace–Young equation) can no longer be supported.

If we now allow liquid vapour, present in the atmosphere to (slowly) condense into the bridge then we expect both triple points to remain “pinned” as both contact angles increase, until $\theta_- = \theta_a$. At this point further addition of liquid will cause the lower triple point to move downward. The net effect is that initially decreasing and then increasing the liquid volume would cause the liquid bridge to move down the substrate; the initial bridge location can never be recovered in this way.

As we then reduce the volume of the bridge both contact angles will decrease. We recall $\theta_+ < \theta_-$. This trend will continue until the upper contact angle reaches the receding value (see

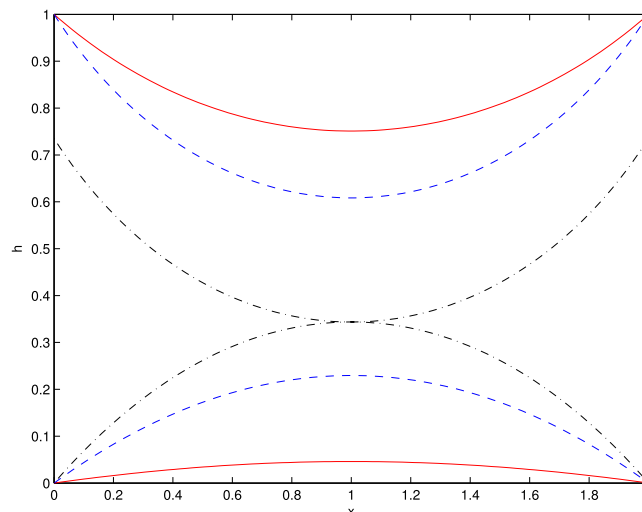


FIG. 6. Evolution of a liquid bridge from a starting position (red) as volume is removed, until the limiting (green) bridge is reached.

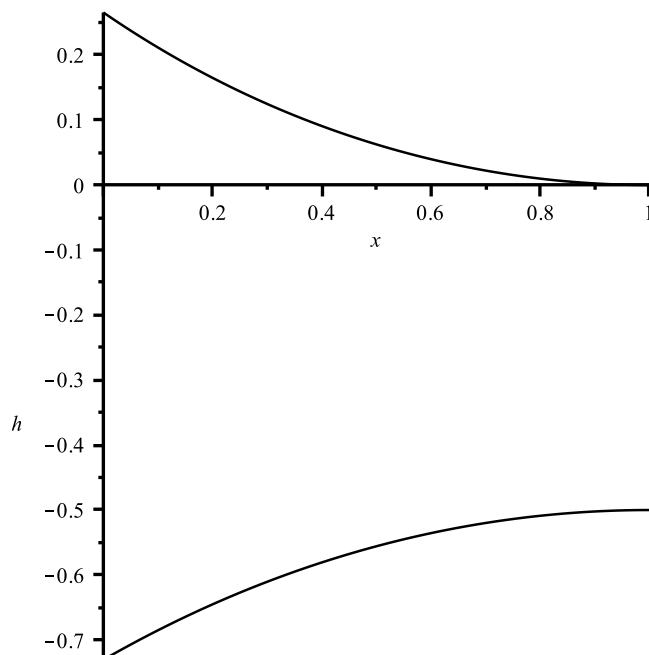


FIG. 7. Initial configuration of bridge.

Figure 3). At this point the upper interface will start to recede while the lower interface will remain pinned. If we continue removing liquid the bridge will reach a limiting situation with $b = 0$, where any further evaporation will presumably cause the bridge to rupture. This limiting volume was discussed in Section IV E. Figure 9 shows such a situation.

We further comment that this process is fundamentally hysteretic. If we consider Figure 9 and allow liquid vapour, present in the atmosphere, to (slowly) condense into the bridge then we expect the upper contact angle to remain fixed while the lower increases until it reaches the advancing

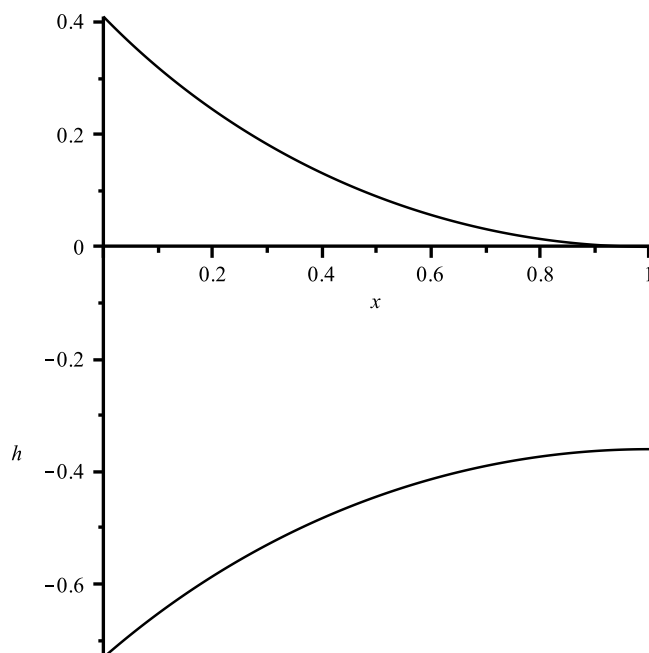


FIG. 8. Bridge as the upper contact angle reaches the receding value.

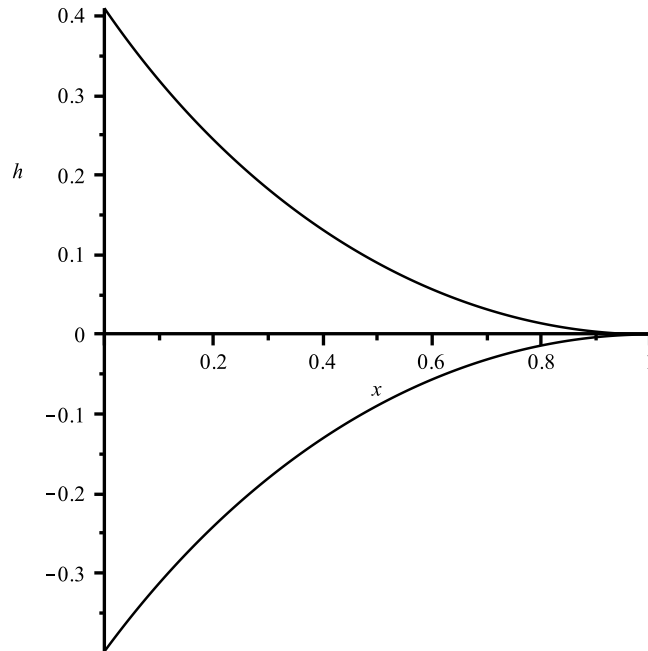


FIG. 9. The limiting bridge. The volume here is approximately 0.2522.

angle (see Figure 3). At this point, further addition of liquid will cause the lower contact line to move downwards. The net effect is that initially decreasing and then increasing the liquid volume would cause the bridge to move down the wall; the initial bridge location can never be recovered in this way.

VII. CONCLUSIONS; FURTHER WORK

The motivation for considering the problem in this paper was the initiation of a study of liquid bridges which arise during the manufacture of stents. (A stent is a tube inserted into a passage in the body to prevent or counteract a disease-induced reduction of flow through the passage.) The stent is made of a superalloy wire, braided in a tubular mesh configuration and covered with a silicone polymer in such a way that it is both flexible and self-expanding. The production of such a stent involves covering the tubular mesh in a highly volatile coating solution. To achieve this the mesh is mounted on a mandrel (a smooth polytetrafluoroethylene cylindrical fixture) (see Figure 10(a))

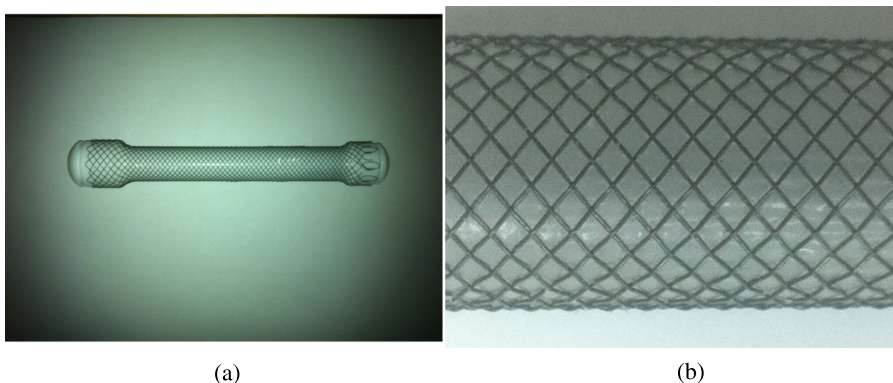


FIG. 10. (a) Stent on mandrel before the curing process. (b) Close up of the final stent, showing the individual “diamonds.”

and both are coated with the solution. After the coating the stent is then cured. During this phase the mandrel and mesh are placed, in the mounted configuration, in an oven at 100 °C for about an hour. In this time, the solvent evaporates and polymerization occurs, causing a steady drop in the volume. It is in this phase of the manufacturing process that, on occasion, a coating defect arises whereby holes can develop in the coating (which forms when the liquid is cured) in one or more of the “diamonds” (see Figure 10(b)). This leads to undesirable wastage as the defect renders the stent unusable.

Each “diamond” can be thought of as supporting a liquid bridge and it is clear that to even find the equilibrium configuration is a challenging problem. In fact, the problem is fully three dimensional, with the added complication that the “walls” supporting each liquid bridge are embedded in a curved surface. In addition, these “walls” are approximately cylindrical in shape which allows for the effective slope of the free liquid surface at the contact line to vary (as the contact line moves around the cylindrical “wall”). Ultimately, the problem is probably only amenable to a numerical approach.

It is thus sensible to first consider a simpler problem with a higher degree of symmetry. Consider one of the “diamonds” in Figure 10(b). We idealise this as a horizontal rectangular frame, comprising four approximately cylindrical or rectangular pillars which support the liquid bridge. If the frame is sufficiently long in one direction, then the section through the bridge in the shorter direction, supported by the cross section of two of the pillars, will be approximately two dimensional. Assuming the frame is long in one direction allows us to neglect effects (or boundary layers) at the ends.

In the present paper, we have thus examined the much simpler problem of determining the shape of a two dimensional liquid bridge supported by two vertical walls and have obtained asymptotic and numerical solutions for the equilibrium configuration, the former in the limit of vanishing Bond number. Unlike previous authors, by avoiding the direct formulation of the problem in terms of the Laplace-Young capillary equation and using a parametric approach, we are able to obtain solutions to first order in the small parameter. While a leading order analysis suggests that equilibrium solutions occur provided the contact angle is fixed and constant, the first order model corrects this result and demonstrates that equilibrium is impossible without contact angle hysteresis, at least in the case where the bridge occurs between two vertical walls. This is confirmed by a global force balance. The situation is similar to that which occurs when a liquid drop is in equilibrium on a flat inclined plane and the upper and lower angles are required to be different in order to balance the weight of the drop.¹⁸ It also verifies, in the appropriate asymptotic limit of vanishing Bond number, the relation between the upper and lower contact angles obtained via an exact force balance. In addition, we formulate a quasi-static model for the configuration of an evaporating film and identify the minimal liquid volume required for the existence of a static bridge (when the upper and lower surfaces are just touching) as determined by the Laplace-Young capillary equation. The next step will be to consider the hydrodynamic and static stability of such a liquid bridge before moving to more geometrically complicated problems.

A further refinement of the model will consider the case where the supporting wires of the frame are approximately cylindrical in shape and the varying inclination of cross section of such wires from the vertical gives rise to additional equilibrium configurations. In addition, we will look at axisymmetric configurations where the supporting frame (cf. the “diamond” of Figure 10(b)) is itself circular and whose component wires are either cylindrical or rectangular in cross section. Ultimately we seek to obtain numerical solutions for the free surface configuration on a real stent and to consider the stability of bridges of this type. We postulate that the occurrence of holes in the liquid bridge in the geometrically more complicated stent problem can be predicted in a manner analogous to the two dimensional and axisymmetric three dimensional cases.

ACKNOWLEDGMENTS

We acknowledge the support of the Mathematics Applications Consortium for Science and Industry (www.macsi.ul.ie) funded by the Science Foundation Ireland Grant investigator Award No. 12/IA/1683.

APPENDIX A: ASYMPTOTIC SOLUTIONS

We seek solutions in the form

$$h_{\pm} = h_{\pm}^{(0)} + B h_{\pm}^{(1)} + B^2 h_{\pm}^{(2)} + O(B^3). \quad (\text{A1})$$

In Subsection A 1 we find leading order solutions for $h_{\pm}^{(0)}$ before attempting to go to the next order and find $h_{\pm}^{(1)}$.

1. Leading order

At leading order we consider only terms that are $O(1)$ so (2.9) yields, for the upper surface

$$-\frac{h_+^{(0)''}}{(1 + h_+^{(0)2})^{\frac{3}{2}}} = P^{(0)}, \quad (\text{A2})$$

with boundary conditions

$$h_+^{(0)'}(0) = -\cot \theta_+, \quad h_+^{(0)'}(1) = 0, \quad h_+^{(0)}(0) = 0.$$

This equation simply states that the curvature is constant, which indicates that the profile is a circular arc. Thus the solution is the lower section of a circle centred at $(1, K)$ with radius K between $x = 0$ and $x = 2$, which can be written as

$$h_+^{(0)} = K - \sqrt{K^2 - (x - 1)^2}, \quad (\text{A3})$$

where $K = 1/P^{(0)}$. Because the profile is symmetric, we require that $\theta_+ = \theta_- \theta$, say. When we also apply the boundary condition $h_+^{(0)'}(0) = -\cot \theta$ we obtain the relationship $P^{(0)} = \cos \theta$. In the same way we find the leading order lower surface is given by

$$h_-^{(0)} = -(b + K) + \sqrt{K^2 - (x - 1)^2}. \quad (\text{A4})$$

2. First order

We now consider terms that are $O(B)$ so (2.9), for the upper surface, yields

$$\left(\frac{-h_+^{(1)''}}{(1 + h_+^{(0)2})^{\frac{3}{2}}} \right) + \left(\frac{3h_+^{(0)'}h_+^{(0)''}}{(1 + h_+^{(0)2})^{\frac{5}{2}}} \right) h_+^{(1)'} = P^{(1)} + h_+^{(0)}, \quad (\text{A5})$$

with the boundary conditions $h_+^{(1)'}(0) = 0$, $h_+^{(1)'}(1) = 0$, and $h_+^{(1)}(1) = 0$. This is essentially a first order ordinary differential equation for $h_+^{(1)'}$, which we can solve and then integrate to find $h_+^{(1)}$. Doing this we obtain the solution

$$\begin{aligned} h_+^{(1)} = & \left(\frac{K^4}{2} - \frac{K^5}{2\sqrt{K^2 - (x - 1)^2}} \right) \arctan \left(\frac{1}{\sqrt{K^2 - 1}} \right) \\ & + \frac{K^3(x - 1)}{2\sqrt{K^2 - (x - 1)^2}} \arctan \left(\frac{x - 1}{\sqrt{K^2 - (x - 1)^2}} \right) \\ & + \frac{K^2}{2} \sqrt{K^2 - 1} - \frac{K^3}{2} \sqrt{\frac{K^2 - 1}{K^2 - (x - 1)^2}}, \end{aligned} \quad (\text{A6})$$

with

$$P^{(1)} = -\frac{1}{2} \sqrt{K^2 - 1} - \frac{1}{2} K^2 \arctan \left(\frac{1}{\sqrt{K^2 - 1}} \right) - K. \quad (\text{A7})$$

If we recall $K = \sec \theta$ we find

$$P^{(1)} = -\frac{1}{2} \tan \theta + \frac{2\theta - \pi}{4} \sec^2 \theta - \sec \theta, \quad (\text{A8})$$

using the identity $\arctan(\cot(\theta)) = -\theta + \pi/2$ for $\theta \in (0, \pi)$. At this stage we note that the algebra is becoming intractable. This will make finding $h_-^{(1)}$, and higher order series solutions, very difficult, if not impossible.

APPENDIX B: FULL SECOND ORDER SOLUTIONS

In the main body of this paper we omitted the value used for $c^{(1)}$, which is

$$\begin{aligned} c^{(1)} = & C (\sin^2 \alpha_+ (\cos \alpha_+ - 2) (\cos^3 \alpha_+ - 4 \cos^2 \alpha_+ - \cos \alpha_+ + 2)) \\ & C (2b \sin^3 \alpha_+ (\cos^3 \alpha_+ - 3 \cos^2 \alpha_+ - \cos \alpha_+ + 2) - b^2 \sin^6 \alpha_+ + 2\alpha_+ b \sin^2 \cos(2\alpha_+)) \\ & C (2\alpha_+ \sin \alpha_+ (2 \cos^3 \alpha_+ - 5 \cos^2 \alpha_+ - \cos \alpha_+ + 2) + \alpha_+^2 (\cos^2 \alpha_+ + \cos(2\alpha_+))), \end{aligned} \quad (\text{B1})$$

where $C = -\frac{1}{2 \cos^3 \alpha_+ \sin^5 \alpha_+}$. And for $V^{(1)}$ we have

$$\begin{aligned} V^{(1)} = & C \{ \sin^2 \alpha_+ (\cos \alpha_+ - 2) (\cos^3 \alpha_+ - 4 \cos^2 \alpha_+ - \cos \alpha_+ + 2) + 2\alpha_+ b \sin^2 \alpha_+ \cos(2\alpha_+) \} \\ & C \{ 2b \sin^3 \alpha_+ (\cos^3 \alpha_+ - 3 \cos^2 \alpha_+ - \cos \alpha_+ + 2) + \alpha_+^2 [\cos^2 \alpha_+ + \cos(2\alpha_+)] \} \\ & C \{ -b^2 \sin^6 \alpha_+ + 2\alpha_+ \sin \alpha_+ (2 \cos^3 \alpha_+ - 5 \cos^2 \alpha_+ - \cos \alpha_+ + 2) \}. \end{aligned} \quad (\text{B2})$$

In the main body on the paper also we omitted the form of the constants used in the second order solutions. Below we list these constants,

$$\begin{aligned} H_{21}^+ = & \frac{\sin^6 \alpha_+}{2} (\cos(2\alpha_+) - 6 \cos \alpha_+ - 3) \\ & + 3\alpha_+ \sin^5 \alpha_+ (2 \cos \alpha_+ - 1) + 3\alpha_+^2 \sin^4 \alpha_+, \end{aligned} \quad (\text{B3})$$

$$\begin{aligned} H_{22}^+ = & -\frac{\sin^6 \alpha_+}{2} (\cos(2\alpha_+) - 7) \\ & - 6\alpha_+ \sin^5 \alpha_+ \cos \alpha_+ - 3\alpha_+^2 \sin^4 \alpha_+, \end{aligned} \quad (\text{B4})$$

$$H_{23}^+ = 3 \sin^6 \alpha_+ \cos \alpha_+ + 3\alpha_+ \sin^5 \alpha_+, \quad (\text{B5})$$

$$H_{24}^+ = -2 \sin^6 \alpha_+, \quad (\text{B6})$$

and the X_{2j}^+ are

$$\begin{aligned} X_{21}^+ = & \frac{3}{4 \sin^6 \alpha_+} (\cos \alpha_+ \sin \alpha_+ + \alpha_+), \\ 4 \sin^7 \alpha_+ X_{22}^+ = & -(6\alpha_+ \cos \alpha_+ \sin \alpha_+ + 3\alpha_+^2) \\ & - \cos^2 \alpha_+ \sin^2 \alpha_+, \\ X_{23}^+ = & -\frac{1}{2 \sin^5 \alpha_+}. \end{aligned}$$

Also on the lower surface we have

$$\begin{aligned} H_{21}^- = & \sin^2 \alpha_+ (\cos \alpha_+ - 2) (\cos \alpha_+ - 10) \\ & + 4b \sin^3 \alpha_+ (\cos \alpha_+ - 5) \\ & + 4\alpha_+ b \sin^2 \alpha_+ + 6\alpha_+ \sin \alpha_+ (\cos \alpha_+ - 2) \\ & + 3\alpha_+^2 + 4b^2 \sin^4 \alpha_+, \\ H_{22}^- = & 3(\cos \alpha_+ - 4) \sin^2 \alpha_+ \\ & + 6b \sin^3 \alpha_+ + 3\alpha_+ \sin \alpha_+, \\ H_{23}^- = & 2 \sin^2 \alpha_+, \end{aligned}$$

$$\begin{aligned}
X_{21}^- &= \cos^4 \alpha_+ - 12 \cos^3 \alpha_+ + \frac{37}{2} \cos^2 \alpha_+ \\
&\quad + 12 \cos \alpha_+ - \frac{39}{2} \\
&\quad - 6\alpha_+ (\cos \alpha_+ - 2) \sin \alpha_+ \\
&\quad + -3\alpha_+^2 - 4b(\cos \alpha_+ - 5) \sin^3 \alpha_+ \\
&\quad - 4b(\alpha_+ + b \sin^2 \alpha_+) \sin^2 \alpha_+, \\
X_{22}^- &= -3(2b \sin^3 \alpha_+ + (\cos \alpha_+ - 4) \sin^2 \alpha_+) \\
&\quad - 3\alpha_+ \sin \alpha_+, \\
X_{23}^- &= -6 \sin^2 \alpha_+.
\end{aligned}$$

- ¹ F. V. Atkinson and L. A. Peletier, "Bounds for vertical points of solutions of prescribed mean curvature equations," *Proc. Roy. Soc. Edinburgh: Sect. A* **112**, 15–32 (1989).
- ² G. K. Batchelor, *An Introduction to Fluid Dynamics* (Cambridge University Press, 1967).
- ³ R. Bhatnagar and R. Finn, "Attractions and repulsions of parallel plates partially immersed in a liquid bath: III," *Boundary Value Probl.* **2013**(1), 277.
- ⁴ E. A. Boucher, "Capillarity phenomena: Properties of systems with fluid/fluid interface," *Rep. Prog. Phys.* **43**, 497–546 (1980).
- ⁵ P. Concus and R. Finn, "The shape of a pendent liquid drop," *Philos. Trans. R. Soc., A* **292**, 307–340 (1978).
- ⁶ R. Finn, *Equilibrium Capillary Surfaces*, Grundlehren der Mathematischen Wissenschaften Vol. 284 (Springer-Verlag, New York, 1986).
- ⁷ R. Finn, "On Young's paradox, and the attractions of immersed parallel plates," *Phys. Fluids* **22**, 017103 (2010).
- ⁸ R. Finn and D. Lu, "Mutual attraction of partially immersed plates," *J. Math. Fluid Mech.* **15**, 273–301 (2013).
- ⁹ P. G. de Gennes, F. Brochard-Wyart, and David Quéré, *Capillarity and Wetting Phenomena: Drops, Bubbles, Pearls, Waves* (Springer, 2004).
- ¹⁰ I. Martinez and J. M. Perales, "Liquid bridge stability data," *J. Cryst. Growth* **78**, 369–378 (1986).
- ¹¹ T. J. McCarthy and L. Gao, "Contact angle hysteresis explained," *Langmuir* **22**, 6234–6237 (2006).
- ¹² S. B. G. O'Brien, "On the shape of small sessile and pendant drops by singular perturbation techniques," *J. Fluid Mech.* **233**, 519–539 (1991).
- ¹³ S. B. G. O'Brien, "Asymptotic solutions for double pendant and extended sessile drops," *Q. Appl. Math.* **52**, 43–48 (1994); available at <http://www.jstor.org/stable/43637970>.
- ¹⁴ S. B. G. O'Brien, "Asymptotics of a pinhole," *J. Colloid Interface Sci.* **191**, 514–516 (1997).
- ¹⁵ S. B. G. O'Brien, "Asymptotics of a series of pendant drops," *SIAM J. Appl. Math.* **62**, 1569–1580 (2002).
- ¹⁶ S. B. G. O'Brien, "Asymptotics of self intersecting solutions of the pendant drop equations," *Z. Angew. Math. Mech.* **84**, 158–170 (2004).
- ¹⁷ S. B. G. O'Brien and B. H. A. A. van den Brule, "Shape of a small sessile drop and the determination of contact angle," *J. Chem. Soc., Faraday Trans.* **87**, 1579–1583 (1991).
- ¹⁸ C. Pozrikidis, "Stability of sessile and pendant liquid drops," *J. Eng. Math.* **72**, 1–20 (2012).
- ¹⁹ L. A. Slobozhanin, J. Meseguer, and J. M. Perales, "A review on the stability of liquid bridges," *Adv. Space Res.* **16**, 5–14 (1995).
- ²⁰ W. Thomson (Lord Kelvin), "Capillary attraction," *Nature* **34**, 270–369, (1886).
- ²¹ T. Young, "An essay on the cohesion of fluids," *Philos. Trans. R. Soc. London* **95**, 65–87 (1805).